Numerical Simulation of the Dynamics of Water Droplet Impingement on a Wax Surface

Junling Hu*[1], Ruoxu Jia[1], Xiao Huang[2], Xingguo Xiong[3], Kai-tak Wan[2]

[1]Department of Mechanical Engineering, University of Bridgeport, Bridgeport, CT 06604 USA
[2]Department of Mechanical and Industrial Engineering, Northeastern University, Boston, MA 02115 USA
[3]Department of Electrical and Computer Engineering, University of Bridgeport, Bridgeport, CT 06604 USA

**jjhu@bridgeport.edu*

Abstract

The impact of droplets on solid surfaces is important for a wide range of engineering applications, such as ink-jet printing, spray cooling of hot surfaces, spray coating and painting, solder-drop deposition, blood spattering for criminal forensics and disease detection, etc. This paper simulated the dynamic process of a water droplet impinging onto a wax substrate in COMSOL, using the Phase Field method for tracking the free surface. The predicted spreading factor and apex height were validated against experimental results, showing good agreement during the dynamic impingement process. The effect of contact angles on the impingement process was also studied. The initial inertia driven spreading process is not affected by the contact angle, but the later spreading process and recoil process are significantly affected by the contact angle. The simulation results can provide a good understanding of the dynamic impingement process and provide insights on how surface wettability can affect the droplet spreading and rebounding process.

Keywords

Droplet impingement, two phase flow, hydrophobic surface, phase field method, contact angle

Introduction

The dynamic behavior of droplet impingement on a solid surface is important to many engineering applications, such as rain drops on automobile windshields, inkjet deposition and metal deposition in manufacturing processes, spray cooling of electronics, and spray coating for various applications. The droplet can spread, splash, and rebound after hitting a solid surface. The resulting phenomena and the final shape of the droplet on a surface depend on several parameters, including the properties of the droplet and the impacted surface, the droplet impact velocity, the droplet size, the angle of attack to the surface, the droplet physical properties, the surface wettability, and surrounding pressure[1]. Impacts of a droplet onto a solid surface are controlled by three key factors: inertia, viscous dissipation and interfacial energy[2,3]. The impact phenomena is characterized by dimensionless numbers[2,3], such as the Weber number ($We = \rho V_i^2 D_0/\sigma$), the Reynolds number ($\mathrm{Re} = \rho \mathrm{V_i} \mathrm{D_0}/\mu$), the Ohnesorge number ($Oh = (We)^{1/2}/Re$), and the Capillary number ($Ca = We/Re$), where ρ is the fluid density, μ is the fluid dynamic viscosity, σ is the surface tension, D_0 is the droplet initial diameter, and V_i is the impact velocity.

Significant research has been dedicated to the study of droplet impingement under various conditions, experimentally, numerically, and analytically[4,5]. Sikalo and Ganic[4] and Sikalo et al.[5] conducted experiments to study the droplet impact of three different fluids on surfaces with various conditions, including dry and wet, smooth and rough, hydrophilic and hydrophobic, and horizontal and inclined. Rein[6], Yarin[7], and Marengo et al.[8] provided comprehensive reviews of droplet impact phenomena under various impacting conditions.

Numerical simulations of droplet impact process can provide insights for the underlying flow physics. Numerical modeling of droplet impact process involves three complexities[9]: (1) tracking the droplet-ambient fluid interface that undergoes extreme deformation in a short time and accounting for the surface tension, (2) resolving the three-phase contact line singularity, and (3) incorporating effects of the surface wettability. Several numerical models were used for interface tracking, including volume of fluid (VOF) method[10,11], Level Set (LS) method[12,13], coupled LS-VOF method (CLSVOF)[14,15], Boundary Element method (BEM)[16], Lattice-Boltzman method (LBM)[17,18], and Phase Field method[19-21]. One of most challenging tasks is to correctly predict the gas–liquid interaction on a three-phase contact line while simultaneously trying to avoid numerical diffusion[10]. Most models apply a contact angle as a boundary condition at the active boundary cells at the wall[10].

Contact angle hysteresis, a difference between the advancing contact angle and receding contact angle, is observed experimentally during the droplet spreading and recoiling process. This dynamic variation of contact angle during the spreading process might be caused by surface inhomogeneity, surface roughness, impurities on the surface and temperature variation[19]. When prescribing the contact angle, the value of the angle is dependent on the sign of the contact-line speed U_{CL} because of hysteresis[22,23]. As it is normally difficult to incorporate a dynamically varying contact angle in computations, a constant contact angle has typically been used. Several works have been devoted to predict the dynamic change of contact angle during the droplet impact process in order to capture the temporal evolution of the phenomenon[10,15,21-24].

The dynamic process of droplet impingement is complex and the mechanism of droplet and surface interaction is not fully understood. This paper investigates the dynamic behavior of a droplet impinging onto a dry wax surface using COMSOL with the Phase Field method. Two different fixed contact angles as well as contact angle hysteresis are studied to see their effects on the droplet impingement process.

Mathematical Model

Assuming that both liquid and gas are Newtonian and the flow is laminar, the flow field can be obtained by solving the Navier-Stokes equations, while the free surface between the two fluids is tracked by the Phase Field method.

The Navier-Stokes equations for the conservation of mass and momentum are formulated as follows:

$$\nabla \mathbf{u} = 0$$

$$\rho\left(\frac{\partial \mathbf{u}}{\partial t} + \mathbf{u}\nabla\mathbf{u}\right) = \nabla\left[-p\mathbf{I} + \mu\nabla\mathbf{u} + (\nabla\mathbf{u})^T\right] + \rho\mathbf{g} + \mathbf{F}_{st}$$

where ρ is the fluid density, $\mathbf{u}$ is the velocity vector, μ is the fluid dynamic viscosity, t is time, p is fluid pressure, $\mathbf{g}$ is the gravitational acceleration, $\mathbf{F_{st}}$ (defined below) is the surface tension force, and $\mathbf{I}$ is the identity matrix.

The Phase Field method is based on the Cahn-Hilliard equation[25], tracking a diffuse surface separating the immiscible phases. The interface is defined by a dimensionless number (ϕ) that

varies from -1 to 1. The 4th order Cahn-Hilliard equation is decomposed into two 2nd order partial differential equations:

$$\frac{\partial \phi}{\partial t} + \mathbf{u}\nabla\phi = \nabla \cdot \frac{\gamma\lambda}{\varepsilon^2}\nabla\psi$$

$$\psi = -\nabla \cdot \varepsilon^2 \nabla\phi - (\phi^2 - 1)\phi$$

where γ is the mobility, λ is the mixing energy density and ε is the interface thickness parameter. The mixing energy density and the interface thickness are related to the surface tension coefficient, σ, through the following relation:

$$\sigma = \frac{2\sqrt{2}\lambda}{3\varepsilon}$$

The mobility determines the time scale of the Cahn-Hilliard diffusion and must be large enough to retain a constant interfacial thickness but small enough so that the convective terms are not overly damped. In COMSOL the mobility is determined by a mobility tuning parameter (χ) that is a function of the interface thickness, $\gamma = \chi\varepsilon^2$. The interfacial thickness is usually taken as the half of the typical mesh size in the region passed by the interface.

The surface tension force is computed as

$$\mathbf{F}_{st} = G\nabla\phi$$

where G is the chemical potential calculated as

$$G = \frac{\lambda}{\varepsilon^2}\psi$$

The volume fractions of the fluids are calculated by

$$V_{fa} = \frac{1-\phi}{2} \quad \text{and} \quad V_{fl} = \frac{1+\phi}{2}$$

The density and viscosity are defined by to vary smoothly across the interface through the definitions

$$\rho = \rho_a + (\rho_l - \rho_a)V_{fl}$$

$$\mu = \mu_a + (\mu_l - \mu_a)V_{fl}$$

where ρ_a, ρ_l, and μ_a, μ_l are the densities and dynamic viscosities of the air and liquid, respectively.

Numerical model

An axisymmetric numerical model is implemented in the commercial finite element software COMSOL 4.3b. The geometry is shown in Fig. 1, where the water droplet is initially positioned at a certain distance above the substrate with an initial velocity. The droplet travels downward toward the substrate under the influence the gravity force and reaches the substrate at an impact velocity V_i.

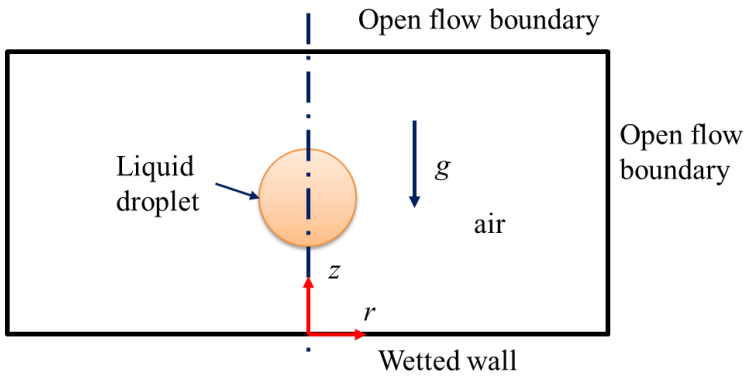

Figure 1. Schematic of axisymmetric computational domain

Open boundary conditions are used at the top and side to simulate an infinite domain. A wetted wall boundary condition is used for the substrate at the bottom. It sets the mass flow across the wall to be zero and specify the contact angle θ_w of fluid at the wall. This is prescribed by

$$\mathbf{n}\cdot\varepsilon^2\nabla\phi = \varepsilon^2\cos(\theta_w)|\nabla\phi|$$

$$\mathbf{n}\cdot\frac{\sigma\lambda}{\varepsilon^2}\nabla\psi = 0$$

As shown in Figure 2, contact angle θ affects the droplet wet diameter d and height h during the droplet spreading process. The spreading factor (d/D_0) is the dimensionless wet diameter at the contact, and the apex height (h/D_0) is the dimensionless droplet height at the centerline, both normalized by the droplet initial diameter D_0.

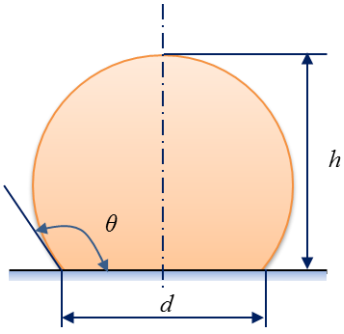

Figure 2. Schematic of droplet attached to a surface: θ, contact angle; h, droplet height; d, droplet wet diameter

Results and Discussion

The paper studied a water droplet of diameter 2.7 mm impinging onto a solid wax surface with an impacting velocity of 1.55 m/s. The material properties of the water droplet and air are listed in Table 1. The Reynolds number, Weber number, Capillary number and Ohnesorge number are

calculated to be Re = 4200, We = 89, Ca = 0.021, and Oh = 0.0023, respectively. According to Shiaffino and Sonin[20,26], the droplet impact behavior in this study is in the regime of hydrodynamic pressure-controlled flow.

The surface wettability of water on a wax surface was characterized by Sikalo and Ganic[4] and Sikalo et al.[5] with static advancing contact angle (θ_a = 105°) and static receding contact angle (θ_r = 95°). However, it is difficult to measure the dynamic contact angles. Therefore, contact angles are varied in the simulation to study their effects on the impingement process. Three different settings of contact angles are used: (1) fixed advancing contact angle (θ_a = 105°) and fixed receding contact angle (θ_r = 95°), and (2)-(3) fixed contact angles (θ = 95° and 100°) unaffected by motion.

Table 1. The properties of water and air

Parameter	Density	Viscosity	Surface tension
	ρ, kg/m^3	μ, Pa·s	σ, N/m
Water	998	0.001	0.073
Air	1.204	1.814×10^{-5}	

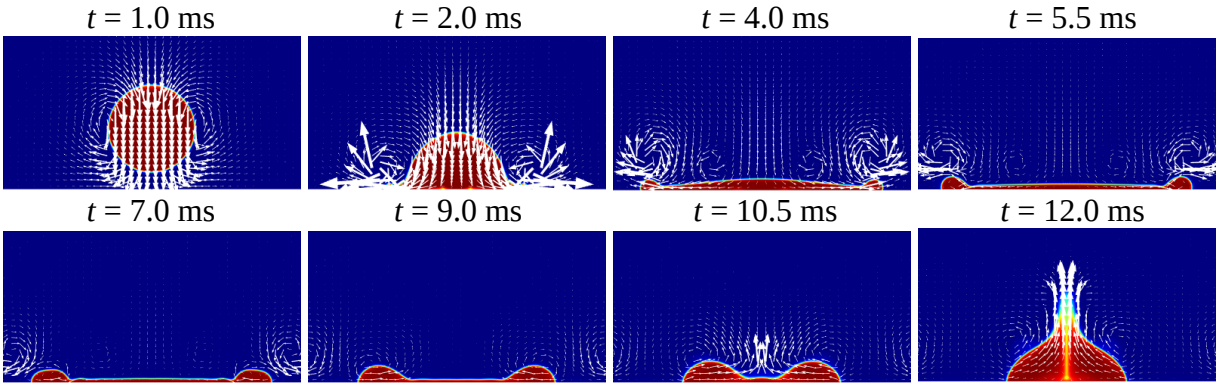

Figure 3. Time sequence of water droplet spreading and initial recoiling obtained with an advancing angle (θ_a) of 105° and a receding angle of (θ_r) of 95°.

Figures 3 and 4 show an evolving sequence of droplet shapes at various time instants simulated with an advancing angle (θ_a) of 105° and a receding angle of (θ_a) of 95°. Velocity vectors are overlaid on the droplet volume fraction contours. It can be seen that the spreading process is driven by the impact pressure and resisted by inertia, and a ring forms at the droplet periphery. The spreading decelerates under the resistance of viscous and capillary forces. Some of the impact energy is dissipated through viscous friction and most of it is stored as surface energy. The droplet reaches its maximum spreading radius around 5.5ms and starts to recoil under the influence of hydrostatic force and capillary force. The central liquid film continues to become thinner, but is still connected to the ring during the spreading and recoiling process. Driven by the capillary force, the ring then begins to move toward the center and contact surface decreases. The ring fluid collides at the center at around 11ms resulting in a large pressure and the liquid starts to move upward. The liquid-solid contact area continues to decrease while the liquid column moves upward and the apex height reaches its maximum at 16.8 ms. The small droplet formed by the fast moving liquid at the top is pulled back into the main liquid column by surface tension, resulting in a temporary setback of the apex height. The fast moving liquid at the top

forms another droplet and the liquid continues to move up to the point where the kinetic energy is largely converted to surface energy. The unstable liquid column then starts to move downward and breaks up at 38.8ms leaving a small amount of liquid behind. The partially rebounded droplet re-contacts the substrate at 40.0ms and combines with the small amount of remnant liquid left at the surface.

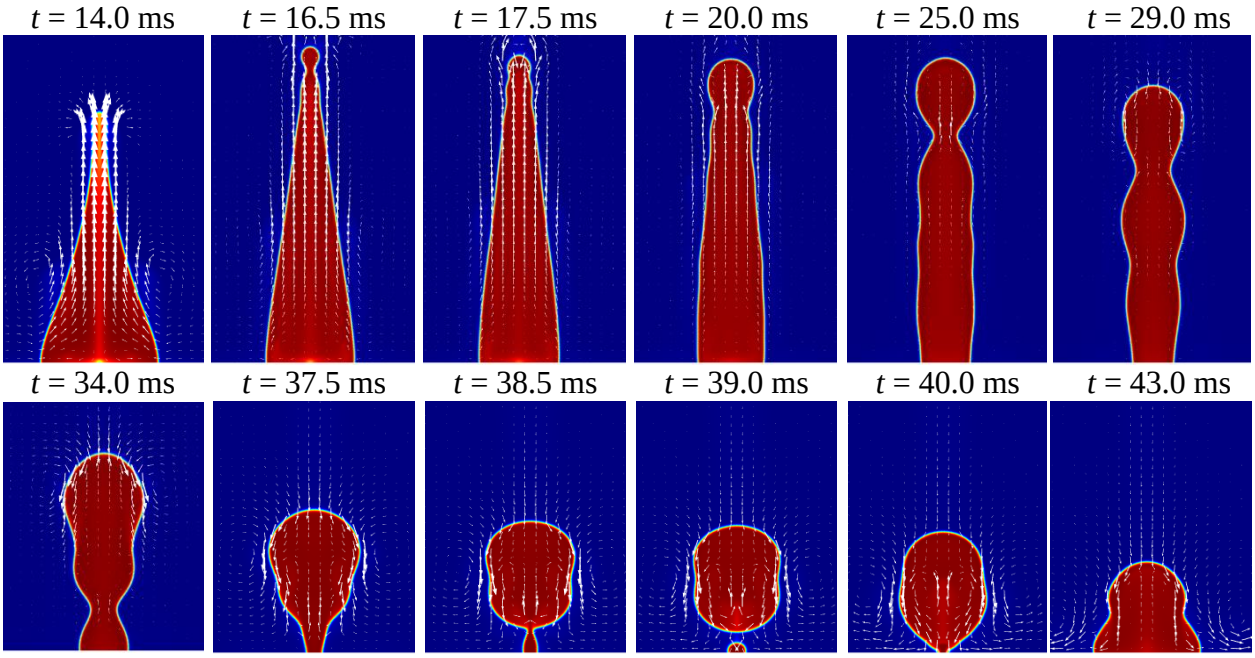

Figure 4. Time sequence of water droplet recoiling process water obtained with an advancing angle (θ_a) of 105º and a receding angle of (θ_r) of 95º.

The changes of spreading factor and apex height during the impingement process can be seen in Figs. 5 and 6, which plot the simulation results obtained with different contact angle settings against the experimental data of Sikalo and Ganic[4] and Sikalo et al.[5] The early spreading process is not affected by the contact angle settings and agrees with the experimental data very well. However, the contact angle affects the maximum spreading and the recoil process. The smaller contact angle leads to a bigger maximum spreading factor.

Sikalo and Ganic[4] and Sikalo et al.[5] observed a small secondary droplet breaking up at around 21ms and another possible bigger droplet breakup near 33ms. Secondary droplet generation is observed in the simulations as well. The first case simulated with an advancing angle (θ_a) of 105º and a receding angle of (θ_r) of 95º predicted the first droplet oscillation near 29ms and the second droplet breakup near 39ms. While the simulation does not predict the breakup of the first droplet and the time of breakup differs, the simulation results capture the whole process well. As shown in Fig. 4, the rebounding process is highly unstable, so it is difficult to predict the exactly the secondary droplet breakups. The recoiling process is found to be highly dependent on the contact angle. As shown in Fig. 5, the simulation with a 95º constant contact angle predicted the first droplet breakup at 26.5ms and the second droplet rebound at 38.3ms. The first droplet size is small and the downward momentum after the first droplet breakup is not strong enough to hold the remnant fluid on the substrate. A second droplet with almost all of the remnant fluids

rebounds for less than 1ms and then returns to the substrate. At a higher contact angle of 100° (Fig. 6) the droplet has a complete rebound at 29ms and the rebound droplet breaks into two droplets at 30.5ms. The sequence of droplet shape evolution in the recoiling process for the 90° and 100° cases can be found in Figs. 7 and 8.

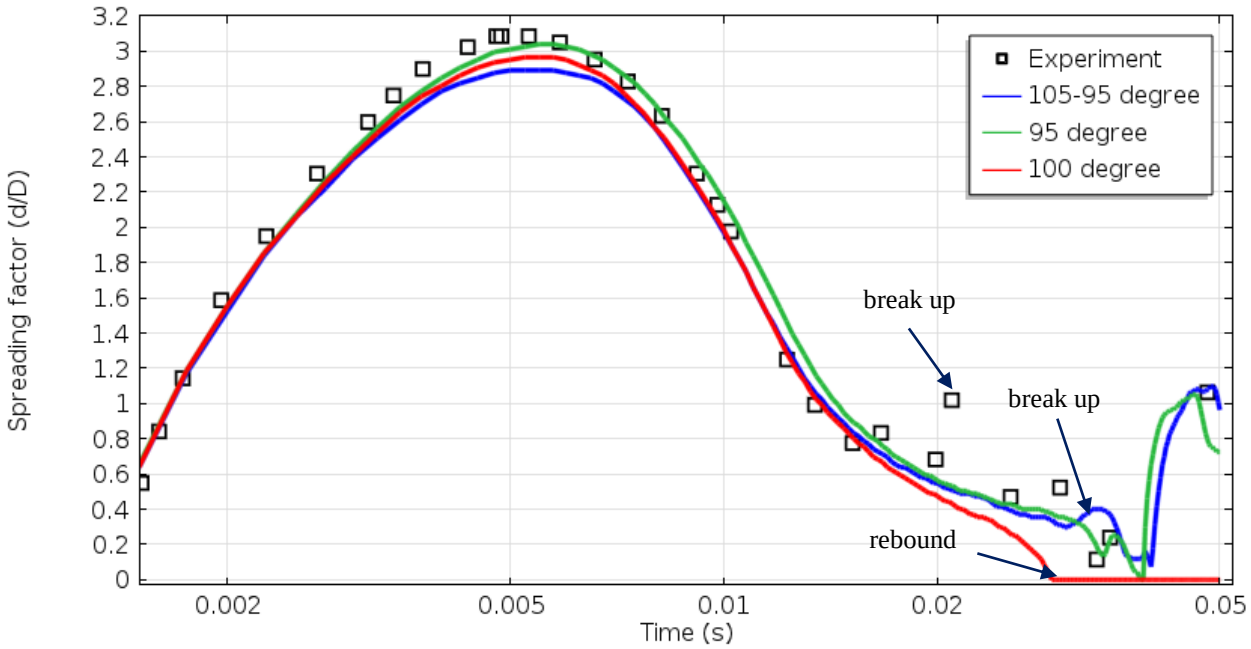

Figure 5. Comparison of simulated spreading factors with the experimental data.

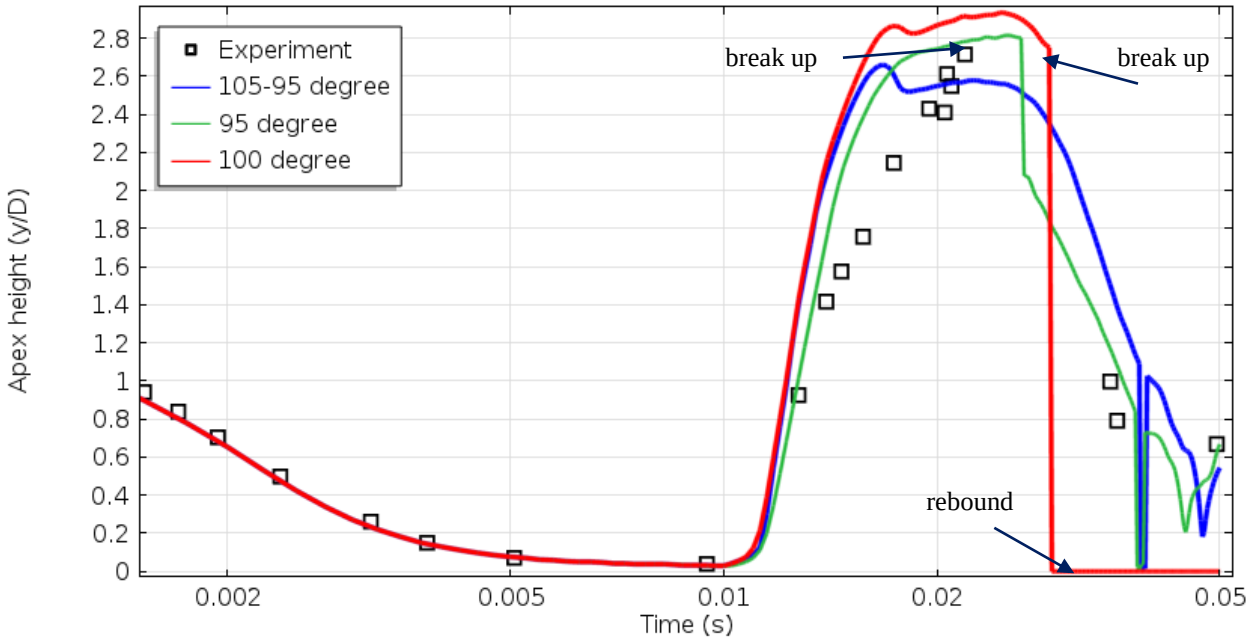

Figure 6. Comparison of simulated apex heights with the experimental data.

Conclusions

This paper simulated the dynamic process of a water droplet impinging onto a wax substrate with the Phase Field method. The dynamic process of droplet evolutions was presented. The predicted spreading factor and apex height were validated against experimental results. The simulation results showed good agreement with the dynamic impingement process found in the experiment. The effect of contact angles on the impingement process was also studied. The initial inertia driven spreading process is not affected by the contact angle, but the later spreading process and recoil process are significantly affected by the contact angle. Higher contact angle during the advance stage lead to a smaller maximum spreading factor and a sooner rebound. The rebound liquid column is unstable with one or two secondary droplet form. The simulation results can provide a good understanding of the dynamic impingement process and provide insights on how to control surface wettability to achieve a desired droplet spreading and rebounding process.

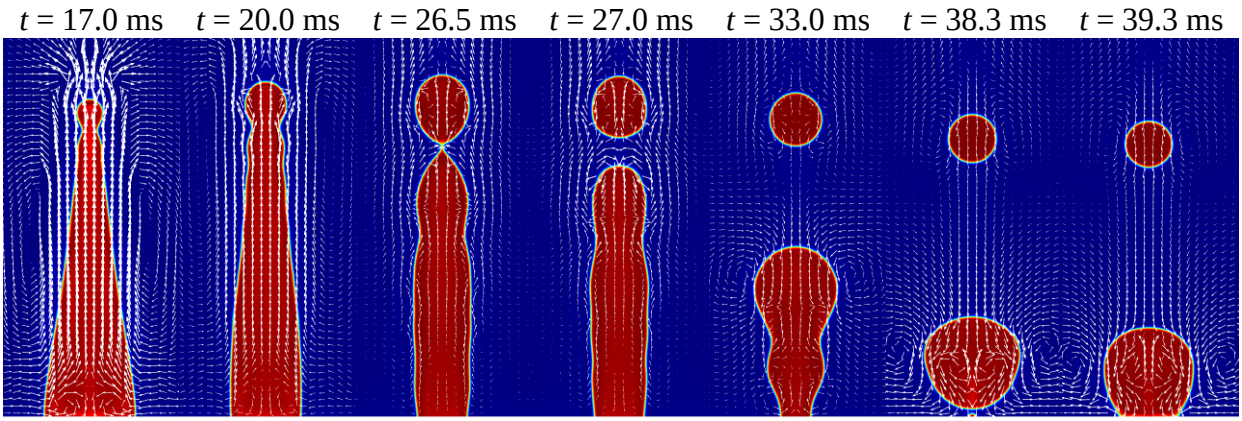

Figure 7. Time sequence of water droplet recoiling process obtained with a constant contact angle of 95^{o}.

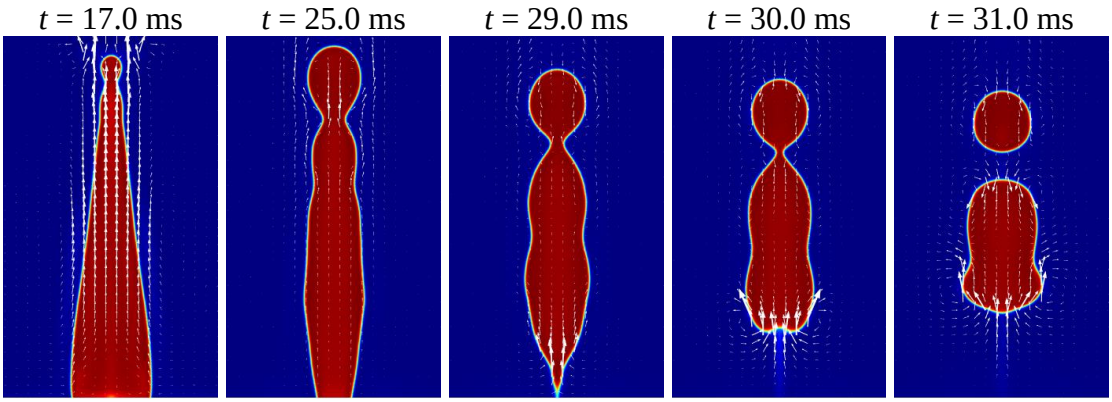

Figure 8. Time sequence of water droplet recoiling process obtained with a constant contact angle of 100^{o}.

References

1. Amit Gupta and Ranganathan Kumar, Droplet impingement and breakup on a dry surface, *Computers and Fluids*, **39**, 1696-1703 (2010).
2. V. Bertola, Dynamic wetting of dilute polymer solutions: the case of impacting droplets, Advances in Colloid and Interface Science, **193-194**, 1-11, 2013.
3. V. Bertola, An impact regime map for water drops impacting on heated surfaces, International J. of Heat and Mass Transfer, **85**, 430-437, 2015.
4. S. Sikalo and E.N. Ganic, Phenomena of droplet-surface interactions, *Experimental Thermal and Fluid Science*, **31**, 97-110 (2006).
5. S. Sikalo, M. Marengo, C. Tropea, and E.N. Ganic, Analysis of impact of droplets on horizontal surfaces, *Experimental Thermal and Fluid Science*, **25**, 503-510 (2002).
6. M. Rein, Phenomena of liquid drop impact on solid and liquid surfaces, Fluid Dyn. Res., **12,** 61–93,1993.
7. A.L. Yarin Drop impact dynamics: splashing, spreading, receding, bouncing. Annu Rev Fluid Mech., **38**, 159–92, 2006.
8. M. Marengo, C. Antonini, I.V. Roisman, C. Tropea, Drop collisions with simple and complex surfaces, Curr Opin Colloid Interface Sci, **16**, 292–302, 2011.
9. V.V. Khatavkar, P.D. Anderson, P.C. Duineveld, H.E.H. Meijer, Diffuse-interface modelling of droplet impact, J. Fluid Mech. **58** (2007) 97-127.
10. I. Malgarinos, N. Nikolopoulos, M. Marengo, C. Antonini, M. Gavaises, VOF simulations of the contact angle dynamics during the drop spreading: standard models and a new wetting force model, Advances in Colloid and Interface Science, **212** (2014) 1-20.
11. N. Nikolopoulos, G. Bergeles, The effect of gas and liquid properties and droplet size ratio on the central collision between two unequal-size droplets in the reflexive regime, Int. J. of Heat and Mass Transfer, **54** (2011) 678-691.
12. J.Hu, R. Jia, K. Wan, X. Xiong, Simulation of droplet impingement on solid surface by the level set method, Proceedings of the COMSOL Conference 2014 Boston, Boston, MA, Oct. 8-10, 2014.
13. S. Tanguy, A. Berlemont, Application of a level set method for simulation of droplet collisions, Int. J. of Multiphase Flow, **31** (2005) 1015-1035.
14. Y. Guo, L. Wei, G. Liang, S. Shen, Simulation of droplet impact on liquid film with CLSVOF, Int. Communications in Heat and Mass Transfer, **53** (2014) 26-33.
15. K. Yokoi, D. Vadillo, J. Hinch, I. Hutchings, Numerical studies of the influence of the dynamic contact angle on a droplet impacting on a dry surface, Physics of Fluids, **21** 072102 (2009).
16. B.H. Bang, S.S. Yoon, H.Y. Kim, S.D. Heister, H. Park, S.C. James, Assessment of gas and liquid velocities induced by an impacting liquid drop, Int. J. of Multiphase Flow, **37**(2011) 55-66.
17. Y. Tanaka, Y. Waashio, M. Yoshino, and T. Hirata, Numerical simulation of dynamic behavior of droplet on solid surface by the two-phase lattice Boltzmann method, *Computers and Fluids*, **40** (2011) 68-78.
18. M. Cheng, J. Lou, A numerical study of splash of oblique drop impact on wet walls, Computer and Fluids, **115** (2015) 11-24.
19. W. Zhou, D. Loney, A. G. Fedorov, F. L Degertekin, D. W. Rosen, Impact of polyurethane droplets on a rigid surface for ink-jet printing manufacturing, 21st Solid Freeform Fabrication Symposium, 2010, Austin, TX.
20. W. Zhou, D. Loney, A. G. Fedorov, F. L Degertekin, D. W. Rosen, Shape evolution of droplet impingement dynamics in ink-jet manufacturing, *22nd Solid Freeform Fabrication Symposium*, Aug.8-10, 2011, Austin, TX.
21. S. Dong, On imposing dynamic contact-angle boundary conditions for wall-bounded liquid-gas flows, Comput. Mehtods Appl. Mech. Engrg., **247-248** (2012) 179-200.
22. P.D.M. Spelt, A level-set approach for simulations of flows with multiple moving contact lines with hysteresis, J. of Computational Physics, **207** (2005) 389-404.
23. Y. Sui, P.D.M. Spelt, An efficient computational model for macroscale simulations of moving contact lines, J. of Computational Physics, **242** (2013) 37-52.
24. A.A. Saha, S.K. Mitra, Effect of dynamic contact angle in a volume of fluid (VOF) model for a microfluidic capillary flow, J. of Colloid and Interface Sci., **339** (2009) 461-480.
25. COMSOL4.3b CFDModuleUserGuide.pdf
26. S. Shiaffino and A.A. Sonin, Molten droplet deposition and solidification at low Weber numbers, *Phys. Fluids*, **9**, 3172-3187 (1997).

Junling Hu

Dr. Junling Hu is an associate professor of Department of Mechanical Engineering at the University of Bridgeport. She received her B.Eng. in Thermal Engineering in 1996 and M.Eng. in Thermal Engineering in 1999 from Huazhong University of Science and Technology and Ph.D. from Missouri University of Science and Technology in 2005.

Ruoxu Jia

Ruoxu Jia is a graduate student of Department of Mechanical Engineering at the University of Bridgeport. He received his B.Eng. at Tianjin Institute of Urban Construction in Safety Engineering in 2012.

Xiao Huang

Xiao Huang is a current Ph.D. candidate at Mechanical & Industrial Engineering at Northeastern University. He obtained his B.Eng. at Beijing Institute of Technology in 2009, and M.S. in Mechanical Engineering at Northeastern University in 2012.

Xingguo Xiong

Dr. Xingguo Xiong is an associate professor of Department of Electrical and Computer Engineering at the University of Bridgeport. He received his BS in Physics from Wuhan University in 1994, Ph.D. in Electrical Engineering from Shanghai Institute of Microsystem and Information Technology, Chinese Academy of Science in 1999 and Ph.D. in Computer Engineering from University of Cincinnati in 2005.

Kai-tak Wan

Kai-tak Wan is a professor at Mechanical & Industrial Engineering at Northeastern University. He obtained his B.Sc. (1st Hon) in Physics at University of New South Wales, Syndey, Australia in 1988, and Ph.D. in Chemical Physics at University of Maryland at College Park in 1993.